No phenotypes in *Ttc22* knockout mice

Running title: *Ttc22* knockout mice

Jiaoyang Liu, Liankun Gu, Abin You, Hongfan Yuan, Jing Zhou, Wei Tian*, Dajun Deng*

Key Laboratory of Carcinogenesis and Translational Research (MOE/Beijing), Division of Etiology, Peking University Cancer Hospital and Institute, Beijing, 100142, China

Corresponding authors: Wei Tian or Dajun Deng, Key Laboratory of Carcinogenesis and Translational Research (MOE/Beijing), Division of Etiology, Peking University Cancer Hospital and Institute, Fu-Cheng-Lu #52, Haidian District, Beijing, 100142, China, Phone:+8610-88196752 (E-mail: tianwei@bjmu.edu.cn or dengdajun@bjmu.edu.cn; ORCID: 0000-0003-2853-7056 or 0000-0001-5161-5943)

Highlights

- Knockout of *Ttc22* exons 2 and 3 completely disrupted gene expression.
- Knockout of *Ttc22* does not affect the development of C57BL mice.
- Knockout of *Ttc22* does not affect the induction of mouse colon cancer by AOM/DSS.

Email address

Jiaoyang Liu, pocky1995@126.com
Liankun Gu, gulkun@163.com
Abin You, youabin115@126.com
Hongfan Yuan, yuanhongfan@scszlyy.org.cn
Jing Zhou, jane72@163.com
Wei Tian, tianwei@bjmu.edu.cn
Dajun Deng, dengdajun@bjmu.edu.cn

ABSTRACT

The *TTC22* gene encodes a protein containing seven tetratricopeptide repeats (TPRs), which mediate protein–protein interactions as chaperones. We previously reported that the level of *TTC22* transcript variant 1 (*TTC22v1*) was downregulated in human colon adenocarcinoma (COAD) and that TTC22 upregulated m6A-mediated *WTAP* and *SNAI1* expression via the TTC22–RPL4 interaction and subsequently promoted COAD metastasis. Thus, a commercially available C57BL/6N mouse model in which the *Ttc22* exon 2&3 encoding the TPR4 (equal to the human TTC22 TPR3) domain was knocked out via CRISPR-Cas9 was used to evaluate the contribution of *Ttc22* to the development of mice and COAD. To determine the status of Ttc22 expression in *Ttc22* knockout mice, we prepared a rabbit polyclonal antibody against the mouse Ttc22 protein, which could bind both wild type Ttc22 and TPR4-deleted Ttc22 proteins overexpressed in HEK293T cells, as determined by Western blot analysis. Ttc22 proteins were detected in colon tissue samples from wild-type mice and *Ttc22* hemi-knockout (*Ttc22*$^{-/+}$) mice but not in those from fully *Ttc22* knockout (*Ttc22*$^{-/-}$) mice. Unfortunately, the long-term observation results demonstrated that *Ttc22* knockout (KO, including *Ttc22*$^{-/+}$ or *Ttc22*$^{-/-}$) did not affect the body weight, development, fertility, or spontaneous tumor incidence of male or female mice. No differences in the incidence of AOM/DSS-induced COAD were observed between these mouse groups, although *Ttc22* deletion partially resulted in the upregulation of genes related to the host adaptive response to inflammation in the colon mucosa. In conclusion, no phenotypes were induced by *Ttc22* inactivation in C57BL/6N mice.

Keywords: Ttc22; TPR4 deletion; C57BL/6N mouse; development; colon cancer; AOM/DSS

42 ## INTRODUCTION

43 The human TTC22 protein contains seven tetratricopeptide repeats (TPRs), which mediate protein–protein
44 interactions and are involved in multiple biological processes, including the movements of cilia and flagella
45 and the migration of human cells [1-5]. A pilot study revealed that the *TTC22* gene was among the top ten
46 downregulated genes in the fetuses of obese women compared with lean women in the second trimester
47 and that low *TTC22* expression in mothers may be related to fetal neurodevelopment and metabolism [6].
48 Differentially methylated regions of the *TTC22* gene are associated with hand grip strength [7]. DNA
49 sequencing and transcriptome data analyses in 3,203 subjects suggested that low-frequency variants of
50 *TTC22* were associated with low-density lipoprotein (LDL) cholesterol [8]. These phenomena imply that
51 TTC22 may be involved in physiological metabolism. However, the causality between TTC22 alterations
52 and metabolism is not known.

53 According to data from the Human Protein Atlas and The Cancer Genome Atlas (TCGA), the *TTC22*
54 gene is comprehensively expressed in epithelial cells in the normal gut mucosa at the middle level and is
55 extensively downregulated in gastrointestinal cancer tissues [9,10]. We initially reported that *TTC22*
56 variant 1 (*TTC22v1*) mRNA is targeted by *miR663a*, an anti-inflammatory miRNA in the colon [11]. *TTC22v1*
57 mRNA expression is significantly lower in human colon adenocarcinoma (COAD) than in paired normal
58 tissue samples, and high *TTC22* expression increases the risk of colon cancer metastasis. Our further study
59 revealed that TTC22 increased m6A-mediated *WTAP* and *SNAI1* expression via TTC22-RPL4 binding and
60 subsequently promoted COAD metastasis *in vitro* and *in vivo* [12], suggesting a potential role for TTC22 in
61 the development and progression of COAD.

62 Therefore, we further studied the effects of Ttc22 on the development of mice and their
63 susceptibility to the chemical carcinogen AOM/DSS via a genetically established and commercially
64 available C57BL gene knockout mouse model in which *Ttc22* exons 2 and 3, which encode the TPR4
65 domain of the mouse Ttc22 protein, were knocked out via CRISPR–Cas9. While qRT-PCR and Western blot
66 analyses confirmed the complete absence of *Ttc22* mRNA and protein in the colon tissues of mice with
67 homozygous deletion of two *Ttc22* alleles (*Ttc22*$^{-/-}$), unexpectedly, no differences in the development,
68 growth, fertility, or AOM/DSS susceptibility of the mice were induced by *Ttc22* knockout. Transcriptomic
69 analysis of colon tissues revealed significant upregulation of genes involved in protein folding and stress
70 response in *Ttc22*$^{-/-}$ mice, indicating that loss of *Ttc22* induces a broad adaptive response that may
71 compensate for its absence. Our findings demonstrate that Ttc22 is dispensable under physiological

72 conditions because of gene redundancy or genetic robustness, highlighting the importance of
73 compensatory mechanisms in gene function studies.

74 MATERIALS AND METHODS

75 *Ttc22* exon 2&3 knockout mouse model

76 Genetically established *Ttc22* knockout (Ttc22-KO) C57BL/6N mice (strain S-KO-06335) were purchased
77 from Cyagen (Cyagen Bio. Co., Guangzhou, China). Ttc22 knockout mice were obtained via
78 high-throughput electroporation of fertilized eggs. The CRISPR-Cas9 system and two gRNAs (gRNA#1:
79 5'-ggaaagugggcauaacgccuggg-3' and gRNA#2: 5'-uuccagagagauagcgaccgagg-3') targeted to *Ttc22* introns
80 1&3 were used to delete a 1610 bp fragment including *Ttc22* exons 2&3 encoding the Ttc22 TPR4 domain
81 (Figure 1A). After sexual maturity, the sperm were collected for cryopreservation. Through hybridization
82 with female wild-type C57BL/6N mice, first-generation Ttc22$^{+/-}$ mice were obtained and used to generate
83 male and female mice with different *Ttc22* genotypes (including Ttc22$^{+/+}$, Ttc22$^{+/-}$, and Ttc22$^{-/-}$), as
84 determined by PCR sequencing via the tail DNA template and two forward primers (OuterF:
85 5'-tcacaacctactcaagatccagc-3' and InnerF: 5'-caactgtagggtatagcagtccc-3') and one common reverse primer
86 (OuterR: 5'-ttattgcctccttggtgagttg-3'). A mouse tissue direct PCR kit (YEASEN, Shanghai, China) was used to
87 amplify *Ttc22*. Both male and female *Ttc22*$^{+/+}$ and *Ttc22*$^{-/-}$ mice were maintained as seed mice in an animal
88 facility under SPF conditions at the Peking University Cancer Hospital & Institute. The seed mice were
89 hybridized to generate experimental mouse stocks with different *Ttc22* genotypes. The body weight of
90 each mouse was measured once a week from 4–31 weeks of age. The animal experiments were approved
91 by the Biomedical Ethical Committee of Peking University Cancer Hospital & Institute.

92 High-fat diet experiment

93 Four-week-old female C57BL/6N mice were consistently fed a high-fat diet, in which 45% of the calories
94 were derived from fat (4.73 kcal/g H10045, Huafukang Bio. Co., Beijing, China). Additionally, a control
95 group of four-week-old female mice was fed a regular diet. The mice were housed in a
96 temperature-controlled room with a 12-h light/dark cycle. All the mice had free access to food and water
97 [13].

98 Fertility test

99 Mating tests were carried out on 6–8-week-old mice. One male Ttc22$^{+/+}$ mouse was mated with 1 Ttc22$^{+/+}$

100 female mouse as the control group, and 1 male Ttc22$^{-/-}$ mouse was mated with 1 Ttc22$^{-/-}$ female mouse as
101 the Ttc22-KO group for the first pregnancy. At least three mates were included in each group. The date and
102 number of pups were recorded at birth in each cage.

103 **Induction of COAD by AOM/DSS**

104 Five male mice aged 6–8 weeks were included in each group within the same cage. The mice in the three
105 groups, *Ttc22*$^{+/+}$, *Ttc22*$^{+/-}$, and *Ttc22*$^{-/-}$ were intraperitoneally administered 10 mg/kg b.w. azoxymethane
106 (AOM) solution (1 mg/mL, freshly prepared with saline; Cat. #A5486 Sigma–Aldrich; Merck KGaA,
107 Darmstadt, Germany) on the 1st experimental day. Beginning on the 2nd experimental day, the mice were
108 administered dextran sodium sulfate (DSS; Cat. #24867; Sigma) in the drinking water containing 2.5% DSS
109 (2.5 g/100 mL) for 7 continuous days. The mice were subsequently allowed to recover for three weeks
110 (drinking water not containing DSS). The combined AOM/DSS treatment cycle was repeated two more
111 times [14]. From the 24th to 27th experimental weeks, the mice were sacrificed, the colon was collected,
112 and the length of the colon was measured. The intestine was opened, and the colon mucosa was carefully
113 examined and photodocumented. Evidence of gross pathologic changes was recorded (e.g., ulceration).
114 Afterward, the colon tissues were fixed with 10% formalin, rolled Swiss, embedded in paraffin, and
115 sectioned for pathological analysis. RNA or protein was extracted from a portion of fresh colon tissue with
116 TRIzol or cell lysis buffer. The remaining tissue was stored at -80°C for subsequent studies. The roll was
117 further fixed in 10% buffered formalin overnight at room temperature and used to prepare tissue sections
118 (4 μm). Pathology was performed by senior pathologists.

119 **RNA sequencing**

120 Total RNA was extracted from the colon tissues of three male mice with different *Ttc22* genotypes via an
121 RNA extraction kit. RNA sequencing was performed by Cloud-Seq Biotech (Shanghai, China). Briefly, total
122 RNA was removed from the rRNAs with an NEBNext rRNA depletion kit (Biolabs, Inc., Massachusetts, USA),
123 which was subsequently used to construct RNA libraries via the NEBNext Ultra II directional RNA library
124 prep kit (Biolabs). Library sequencing was performed on an Illumina NovaSeq 6000 instrument with 150 bp
125 paired-end reads. Paired-end reads were subsequently harvested. The high-quality clean reads were
126 aligned to the reference genome with HISAT2 software (v2.0.4), guided by the Ensembl gtf gene
127 annotation file, and the gene level FPKM was obtained as the expression profile of the mRNAs. Fold
128 changes and p values were calculated on the basis of the FPKM values, and the differentially expressed

129 mRNAs were identified on the basis of |log(FC)|>=1.0 and a p value<= 0.05. GO and pathway enrichment
130 analyses were performed on the differentially expressed mRNAs. The raw data were deposited under the
131 Gene Expression Omnibus accession number GSE275363.

132 **m6A dot blot analysis**

133 m6A dot blot analysis was performed as we previously reported [12].

134 **Quantification of m6A abundance via m6A-specific ELISA**

135 The total RNA m6A level was quantified with an EpiQuik m6A RNA Methylation Quantification Kit (P-9005;
136 Epigentek Group, NY, USA) according to the manufacturer's instructions [15,16].

137 **LC–MS/MS measurement of the m6A/rA ratio**

138 Liquid-MS/MS quantification of m6A was performed by Cloudseq Biotech, Inc. (Shanghai, China), as
139 described previously [12].

140 **Full-length Ttc22, ΔTPR1, and ΔTPR4 expression vectors**

141 The pCMV6-Flag full-length Ttc22 expression vector was purchased from the MiaoLing Plasmid Platform
142 (Wuhan, China) [12]. The ΔTPR4 vector not containing 568-738 bp and the ΔTPR1 vector not containing
143 4-297 bp were derived from the full-length Ttc22 vector and confirmed by Sanger sequencing (Figure
144 S1-S3). These vectors were used to transiently transfect human colon cancer HEK293T cells (ATCC;
145 Manassas, VA, USA).

146 **Western blot analysis**

147 Cells were harvested 48 hrs after transfection and in 1× cell lysis buffer [50 mmol/L Tris-HCl (pH 6.8), 100
148 mmol/L DTT, and 2% SDS. 0.1% bromophenol blue and 10% glycerol] was used to extract total cellular
149 proteins. Protein electrophoresis was performed using 10% SDS-PAGE gels. The membranes were
150 incubated with the following primary antibodies at 4°C overnight: a mouse anti-DYKDDDDK Flag
151 monoclonal antibody (1:3000; cat. no. 66008-4-Ig, Proteintech Group, Inc. Wuhan, China), a mouse
152 anti-Gapdh monoclonal antibody (1:10000; cat. no. 60004-1-Ig; Proteintech Group, Inc., Wuhan, China),
153 and a rabbit anti-His-TTC22 (1-569 aa) polyclonal antibody previously raised and characterized in our own
154 laboratory [12]. The membranes were subsequently incubated with horseradish peroxidase
155 (HRP)-conjugated anti-rabbit or anti-mouse secondary antibodies (1:5000; cat.no. A0208 or A0216,

156 Beyotime Technology, Shanghai, China) at room temperature for 50 min.

157 Mouse colon tissue was collected and homogenized in a 1.5 mL microcentrifuge tube. Afterward, 1
158 mL of lysis buffer was added per 50 mg of tissue. The remaining steps were carried out as described above
159 for the cell samples.

160 **Statistical analysis**

161 Statistical analysis was carried out via SPSS 22. 0 software (SPSS Inc., Chicago IL, USA). The data are
162 presented as the means ± SDs of at least three independent experiments or as the medians (25th–75th
163 percentiles). Statistical analysis methods included Student's t test, one-way analysis of variance (ANOVA),
164 and two-way ANOVA. The exact statistical methods are described in detail for each experiment in the
165 Results section. All tests were two-sided. A p value <0.05 was considered to indicate statistical
166 significance.

167 ## RESULTS

168 **Characterization of *Ttc22* genotypes**

169 To evaluate the effects of the *Ttc22* gene on the development of mice and COAD, a commercially available
170 heterozygous Ttc22-KO C57BL/6N mouse model was used to generate mice with various *Ttc22* genotypes,
171 including homozygous and heterozygous Ttc22-KO ($Ttc22^{-/-}$ and $Ttc22^{+/-}$) and its wild-type control ($Ttc22^{+/+}$)
172 mice, as described in the Methods section. The sequencing results indicated that a 1610 bp fragment,
173 including *Ttc22* exons 2 and 3, which encode the Ttc22 TPR4 domain (57 aa), was deleted via CRISPR-Cas9
174 and two gRNAs (Figure 1A and 1B). RNA sequencing confirmed the sequencing results (Figure 1C).

175 To determine the expression level of the Ttc22 protein in the colons, we performed Western blot
176 analysis using a rabbit polyclonal antibody against human TTC22 previously created at our laboratory [12].
177 We initially investigated whether the TTC22 antibody might also bind mouse Ttc22 and found that the
178 TTC22 antibody efficiently bound both wild-type Flag-Ttc22 and its ΔTPR1 and ΔTPR4 variants (Figure 2A
179 and Figure S1-S3) overexpressed in HEK293T cells by Western blotting (Figure 2B). These results were
180 consistent with those obtained with the anti-Flag antibody. However, Ttc22 was detected only in the colon
181 tissues from $Ttc22^{+/+}$ and $Ttc22^{+/-}$ male mice, and no Ttc22 was detected in the colon tissues from $Ttc22^{-/-}$
182 mice (Figure 2C), indicating complete loss of Ttc22 expression in the colon. We further checked the
183 knockout status of the *Ttc22* alleles in the colon tissues from these mice. To simultaneously amplify both
184 wild-type *Ttc22* and its exon 2&3-deleted variant by the same PCR, we pooled three primers (OuterF,

185 InnerF, and OuterR) together. As expected, the 828 bp PCR products were amplified only by OuterF and
186 OuterR primers from the genetic DNA of *Ttc22*$^{-/-}$ and *Ttc22*$^{+/-}$ mice and were not amplified from the
187 genetic DNA of *Ttc22*$^{+/+}$ mice (1610 bp + 828 bp = 2438 bp; too long to be amplified). In contrast, the 568
188 bp PCR products were amplified only by the InnerF and OuterR primers in *Ttc22*$^{+/+}$ and *Ttc22*$^{+/-}$ male mice
189 and not in *Ttc22*$^{-/-}$ mice (Figure 1D). Collectively, these results indicate that only *Ttc22* exons 2 and 3 are
190 knocked out in these mice, which leads to complete loss of Ttc22 expression.

191 **No morphologic alterations in heterozygous and homozygous Ttc22-KO mice**

192 Compared with wild-type C57BL/6N mice, those with different *Ttc22* knockout states did not differ in
193 development, growth, appearance (Figure 3), body weight (Figure 4A and 4B), or fertility (Figure 5).

194 Considering that *TTC22* is mostly downregulated in the fetuses of obese women and that
195 low-frequency variants of TTC22 are associated with low-density lipoprotein (LDL) cholesterol in the
196 human body [1,3], we further compared the body weights of female *Ttc22* mice fed a high-fat diet.
197 However, no differences in the body weights of C57BL/6N mice in different *Ttc22* genotype groups were
198 observed (Figure 4C).

199 No spontaneous tumors were observed in these mice up to 40 weeks of age. As expected,
200 spontaneous tumors, including lymphoma, sebaceous carcinoma, and basal carcinoma, occurred in some
201 old mice. However, no differences in the incidence of spontaneous tumors were detected between these
202 *Ttc22* genotype groups (Table 1).

203 **No differences in AOM/DSS-induced COAD between** *Ttc22*$^{+/+}$, *Ttc22*$^{+/-}$, and *Ttc22*$^{-/-}$ **mice**

204 Because *TTC22* is involved in COAD development and metastasis [5,6], we wondered whether Ttc22-KO
205 might affect the development of COAD induced by three cycles of AOM/DSS treatment in male mice. By
206 the end of the 24th or 27th experimental week, well-differentiated or moderately differentiated
207 adenocarcinomas were induced in the colons of all AOM/DSS-treated mice but not in those of the 0.9%
208 NaCl control mice (Figure 6). The AOM/DSS-induced tumor burden in *Ttc22*$^{+/+}$ mice was heterogeneous,
209 ranging from multiple small nodules to a large tumor (d =1 cm). Similar phenomena were also observed in
210 *TTC22*$^{+/-}$ mice, with one animal harboring a very large tumor (d=1.8 cm). Two of the five AOM/DSS-treated
211 *Ttc22*$^{-/-}$ mice experienced fatalities during the experimental period. However, no differences in the
212 incidence or severity of colorectal tumors were observed between these mouse groups.
213

214 **Changes in genome-wide adaptive gene expression in the colon of Ttc22-KO mice**

215 We performed RNA sequencing on total RNA extracted from the colons of three 58-week-old male
216 mice with different *Ttc22* genotypes. A total of 528 genes were differentially expressed ($|\log(FC)|\geq 1$ and
217 $p\leq 0.05$) upon *Ttc22* knockout, comprising 303 upregulated genes and 225 downregulated genes. The
218 results of the GO and pathway analyses revealed that *Ttc22* knockout resulted in the upregulation of
219 genes related to infection by microorganisms (Figure 7).

220 We previously reported that TTC22 increases total RNA m6A modification through RPL4-mediated
221 WTAP upregulation [12]. Interestingly, no significant difference in the total RNA m6A level was observed in
222 the colons between these groups of mice with different *Ttc22* genotypes (Figure 8).

223 The above results imply that Ttc22 may contribute to host defense responses against various
224 infections and colon cancer development and that *Ttc22* knockout induces a broad adaptive response that
225 may compensate for its absence.

226 DISCUSSION

227 Considering that *TTC22* mediates human COAD metastasis [11,12], we studied the influence of *Ttc22*
228 knockout on the development of COAD in C57BL/6N mice. Unfortunately, no significant differences in the
229 development or fertility of mice and AOM/DSS-induced COAD were observed between wild-type and
230 Ttc22-KO C57BL/6N mice, although deletion of the Ttc22 TPR4 domain fully disrupted *Ttc22* expression in
231 mice and the mechanism underlying this disruption is unknown.

232 The AOM/DSS-mediated COAD model is a conventional and efficient model for studying
233 inflammation-driven colon carcinogenesis in a controlled experimental timeframe. *TTC22* mRNA is a key
234 target of *miR663A*, a miRNA that acts against inflammation during the development and progression of
235 colon cancer [10, 11]. Therefore, we tested whether loss of function of *Ttc22* affects AOM/DSS-induced
236 colon carcinogenesis in mice. We found that the incidence of colon cancer was similar in all of these mice
237 treated with AOM/DSS. We detected no significant difference in the level of total RNA m6A modification in
238 colon tissues from these mice with various *Ttc22* genotypes. This may account for the lack of difference in
239 the prevalence of AOM/DSS induction between these mouse groups. In the current study, we cannot
240 exclude the possibility that the doses of AOM and DSS administered were too high to display the effects of
241 *Ttc22* inactivation. TTC22 is a scaffold protein. It is unknown where other redundant scaffold proteins may
242 functionally compensate for defects in Ttc22 expression.

In conclusion, we report that deletion of the Ttc22 TPR4 domain disrupts Ttc22 expression and does not induce abnormal phenotypes in mice, including development, growth, or COAD induction by AOM/DSS.

Abbreviations

COAD, colon adenocarcinoma

Ttc22, tetratricopeptide repeat domain 22

AOM, azoxymethane

DSS, dextran sodium sulfate

m6A, N6-methyladenosine

LDL, low-density lipoprotein

TCGA, The Cancer Genome Atlas

Ttc22-KO, Ttc22 knockout

SPF, specific pathogen-free

FPKM, fragments per kilobase of transcript per million mapped reads

FC, Fold Change

GO, Gene Ontology

LC-MS/MS, liquid chromatography–tandem mass spectrometry

NC, negative control

PC, positive control

DTT, dithiothreitol

SDS-PAGE, sodium dodecyl sulfate–polyacrylamide gel electrophoresis

PBS, phosphate-buffered saline

SD, standard deviation

Funding This work was supported by grants from the Beijing Hospital Authority Mission Plan (SML20191101) to DD and from the Science Foundation of Peking University Cancer Hospital (grant #2022-8) to TW.

Author contributions

Conceptualization: DJD, WT, ABY; Funding acquisition: DJD; Investigation: JYL, WT, LKG, ABY, HFY, JZ;

271 Methodology: WT; Project administration: DJD and WT; Visualization: DJD and WT; Writing – original draft:
272 JYL, WT, and DJD; Writing – review & editing: all authors

273 Competing interest

274 The authors declare that they have no competing interests.

275 Acknowledgments

276 We acknowledge the support from Beijing Hospital Authority and Peking University Cancer Hospital for
277 this project. We also extend our gratitude to staff from the laboratory animal center at Peking University
278 Cancer Hospital for their care and maintenance of the animals.

279 REFERENCE

280 1. D'Andrea, L. TPR proteins: the versatile helix. *Trends in Biochemical Sciences*, 2003. 28(12): 655-662.
281 2. Hesketh SJ, Mukhopadhyay AG, Nakamura D, Toropova K, Roberts AJ. IFT-A structure reveals
282 carriages for membrane protein transport into cilia. Cell, 2022. 185(26): 4971-4985.e16.
283 3. Shamoto N, Narita K, Kubo T, Oda T, Takeda S. CFAP70 Is a Novel Axoneme-Binding Protein That
284 Localizes at the Base of the Outer Dynein Arm and Regulates Ciliary Motility. Cells, 2018. 7(9): p. 124.
285 4. Vomastek T, Iwanicki MP, Burack WR, Tiwari D, Kumar D, Parsons JT, Weber MJ, Nandicoori VK.
286 Extracellular signal-regulated kinase 2 (ERK2) phosphorylation sites and docking domain on the
287 nuclear pore complex protein Tpr cooperatively regulate ERK2-Tpr interaction. Mol Cell Biol. 2008
288 Nov;28(22):6954-66.
289 5. McCloskey A, Ibarra A, Hetzer MW. Tpr regulates the total number of nuclear pore complexes per
290 cell nucleus. Genes Dev. 2018 Oct 1;32(19-20):1321-1331.
291 6. Edlow AG, Vora NL, Hui L, Wick HC, Cowan JM, Bianchi DW. Maternal obesity affects fetal
292 neurodevelopmental and metabolic gene expression: a pilot study. PLoS One, 2014 Feb
293 18;9(2):e88661.
294 7. Soerensen, M. *et al.* Epigenome-wide exploratory study of monozygotic twins suggests differentially
295 methylated regions to associate with hand grip strength. Biogerontology, 2019;20, 627-647.
296 8. Yang T, Wu C, Wei P, Pan W. Integrating DNA sequencing and transcriptomic data for association
297 analyses of low-frequency variants and lipid traits. Hum Mol Genet. 2020 Feb 1;29(3):515-526.
298 9. Uhlén M, Fagerberg L, Hallström BM, Lindskog C, Oksvold P, Mardinoglu A, Sivertsson Å, Kampf C,

299 Sjöstedt E, Asplund A, et al: Proteomics. Tissue-based map of the human proteome. Science, 2015,
300 347:1260419.
301 10. Cerami E, et al. The cBio cancer genomics portal: an open platform for exploring multidimensional
302 cancer genomics data. Cancer Discov. 2012, 2:401-404.
303 11. Tian W, Du Y, Ma Y, Zhang B, Gu L, Zhou J, Deng D. miR663a-TTC22V1 axis inhibits colon cancer
304 metastasis. Oncol Rep. 2019 Mar;41(3):1718-1728.
305 12. You A, Tian W, Yuan H, Gu L, Zhou J, Deng D. TTC22 promotes m6A-mediated WTAP expression and
306 colon cancer metastasis in an RPL4 binding-dependent pattern. Oncogene, 2022
307 Aug;41(32):3925-3938.
308 13. Nakamura Y, Natsume M, Yasuda A, Ishizaka M, Kawahat K, Koga J. Fructooligosaccharides suppress
309 high-fat diet-induced fat accumulation in C57BL/6J mice. Biofactors, 2017. 43(2): p. 145-151.
310 14. Angelou A, Andreatos N, Antoniou E, Zacharioudaki A, Theodoropoulos G, Damaskos C, Garmpis N,
311 Yuan C, Xiao W, Theocharis S, Zografos G, Papalois A, Margonis GA. A Novel Modification of the
312 AOM/DSS Model for Inducing Intestinal Adenomas in Mice. Anticancer Res. 2018
313 Jun;38(6):3467-3470.
314 15. Xu Y, Zhou J, Li L, et al. FTO-mediated autophagy promotes progression of clear cell renal cell
315 carcinoma via regulating SIK2 mRNA stability. Int J Biol Sci. 2022; 18(15):5943-5962.
316 16. Ren QW, Xiang MY, Qiao JL, Liu ZJ, Zhang G, Gu LK, Zhou J, Tian W, Deng DJ. TTC7B triggers the
317 PI4KA-AKT1-RXRA-FTO axis and inhibits colon cancer cell proliferation by increasing RNA methylation.
318 Int J Biol Sci. 2025; 21(3):1127-1143.
319

320 ## FIGURES AND LEGENDS

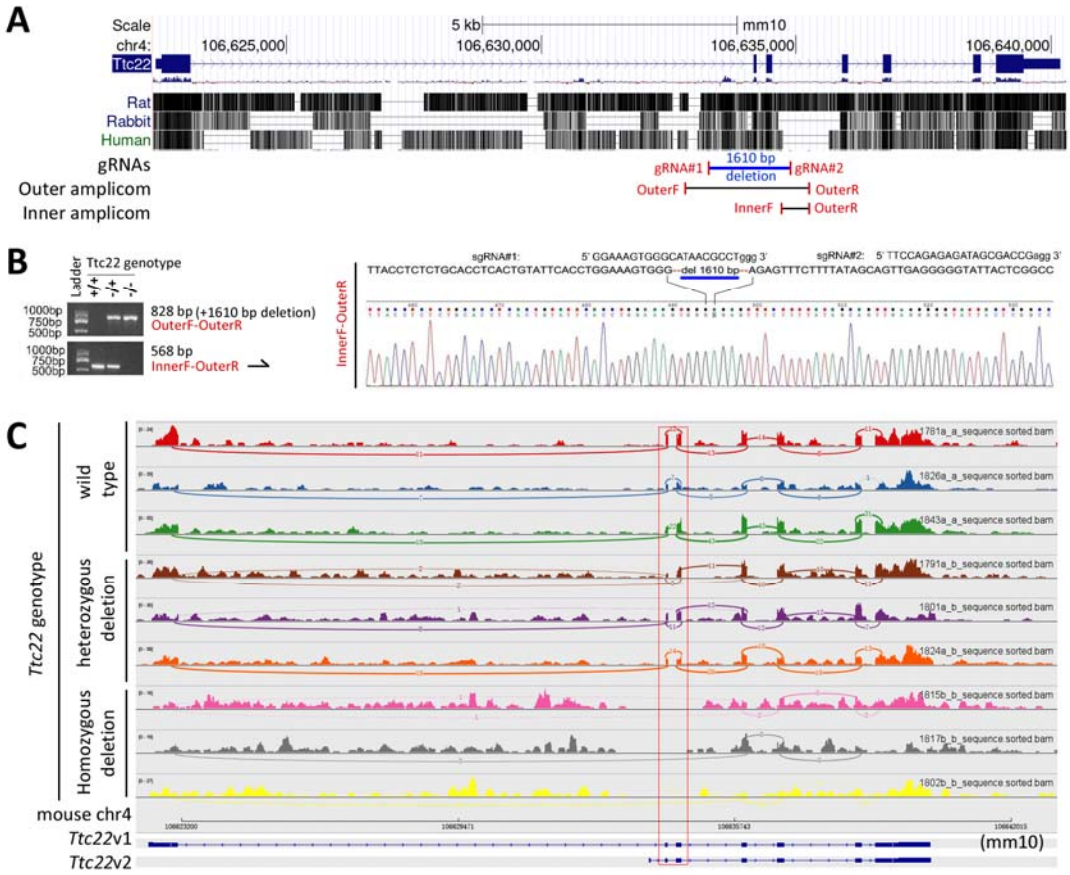

321

322 **Figure 1**. Characterization of the genotypes of the *Ttc22* gene in C57BL/6N mice via CRISPR-Cas9. (**A**)
323 Locations of the deleted fragment (1610 bp), amplicons, gRNAs, and primers matched to the *Ttc22*
324 gene. The conservation status of *Ttc22* in placental mammals, including rats, rabbits, and humans, is
325 displayed below. (**B**) Characterization of *Ttc22* genotypes, as determined by PCR and sequencing.
326 The wild-type *Ttc22* fragment is too long (2438 bp) to be amplified via regular PCR via the OuterF
327 and OuterR primer sets. (**C**) IGV view of *Ttc22* transcripts in RNA samples from the colons of three
328 male mice with different *Ttc22* genotypes, namely, *Ttc22* wild-type ($Ttc22^{+/+}$), heterozygously
329 deleted ($Ttc22^{-/+}$), and homozygously deleted ($Ttc22^{-/-}$) strains, as determined by RNA sequencing.
330 The exon 2&3 region, which is shared by both *Ttc22* variants 1 and 2 and is knocked out by
331 CRISPR-Cas9, is highlighted by a red rectangle.

332

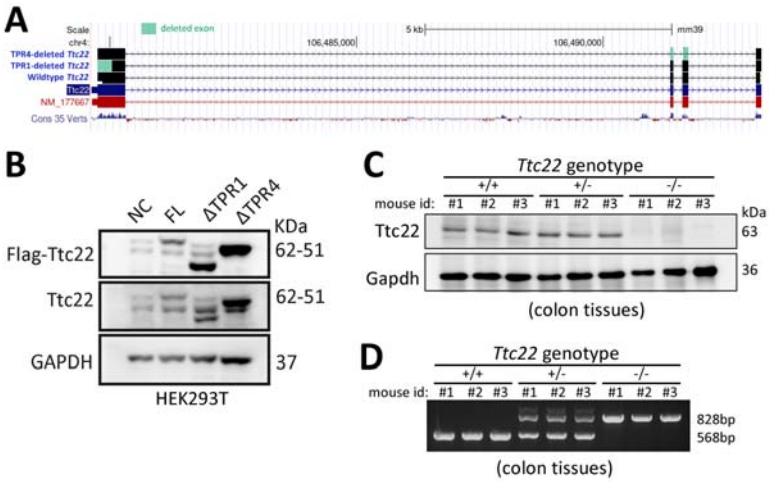

Figure 2. Characterization of the knockout status of the *Ttc22* gene in the mouse colon. (**A**) Illustration of wild-type *Ttc22* and its TPR1- or TPR4-deleted (ΔTPR1 or ΔTPR4) expression vectors. (**B**) Western blot images of the full-length (FL)/wild-type Ttc22 protein and its ΔTPR1 or ΔTPR4 variant overexpressed in HEK293T cells. (**C**) The abundance of the Ttc22 protein in mouse colon tissues from three groups of mice, as determined by Western blotting. (**D**) Characterization of *Ttc22* genotypes in mouse colon tissues, as determined by PCR via a pooled primer set, including OuterF, InnerF, and OuterR.

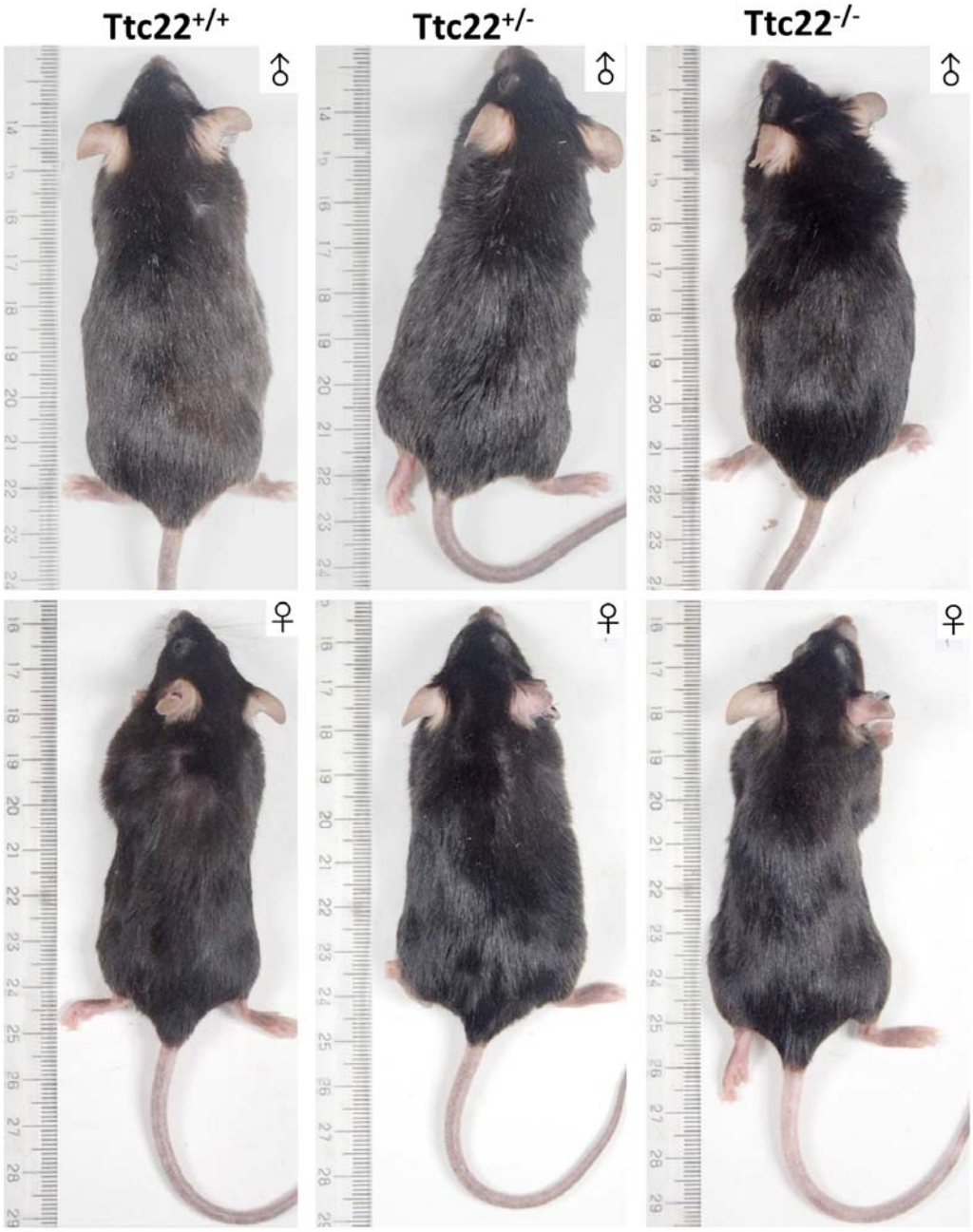

Figure 3. The appearance of C57BL/6N male and female C57BL/6N mice with different *Ttc22* genotypes at approximately 66 and 77 weeks of age

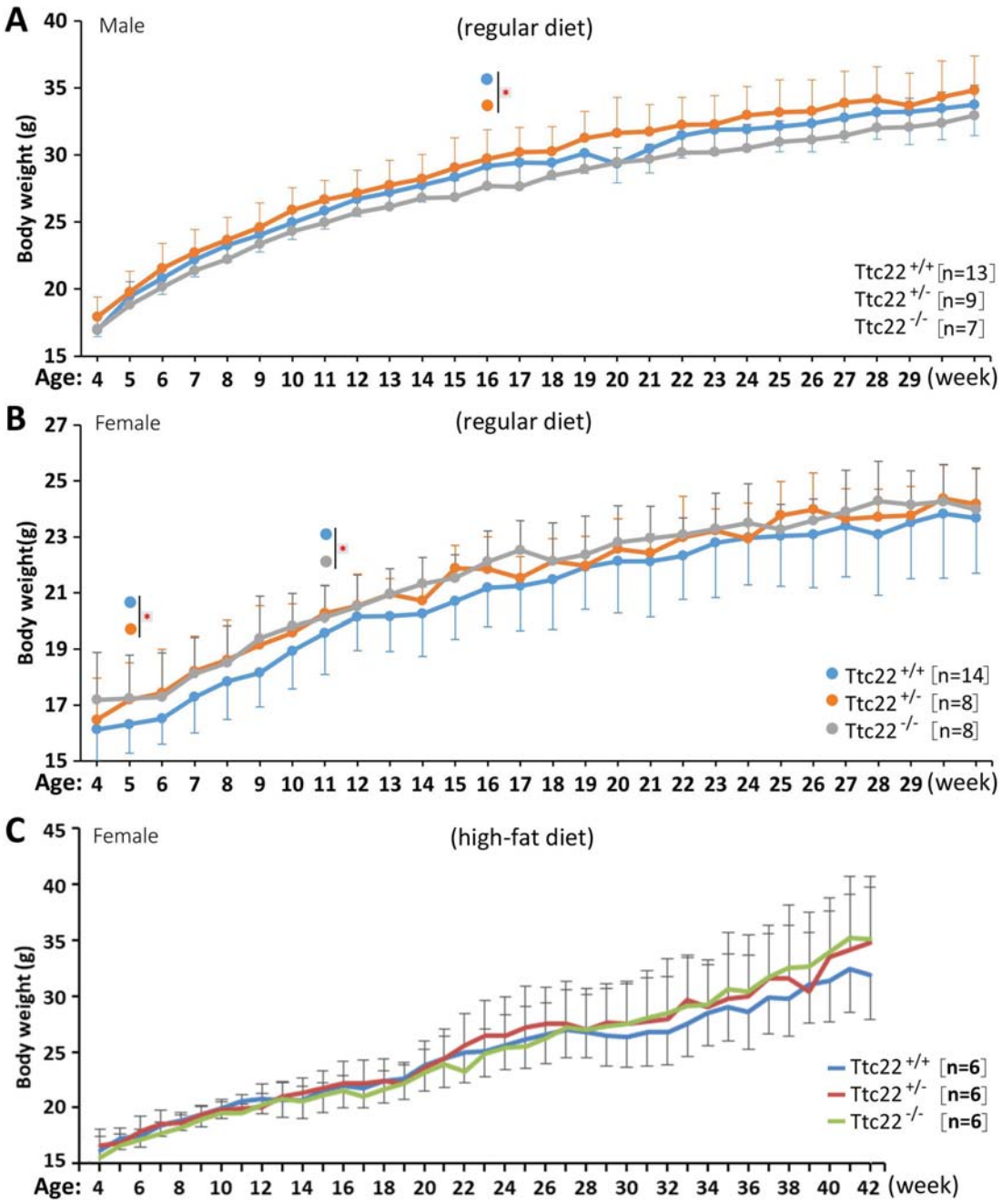

Figure 4. Body weight curves of C57BL/6N mice in different *Ttc22* genotype groups fed a regular or high-fat diet. (**A** and **B**) Body weight curves for male and female mice fed a regular diet. *p<0.05 between groups was observed only on three days (the 16th week for males and the 5th and 11th weeks for females) during 31 experimental weeks, according to Student's t test. (**C**) Body weight curves for female mice fed a high-fat diet. The dots and bars represent the mean values and standard deviations (SDs) of the body weights of the mice. *p<0.05 according to Student's t test.

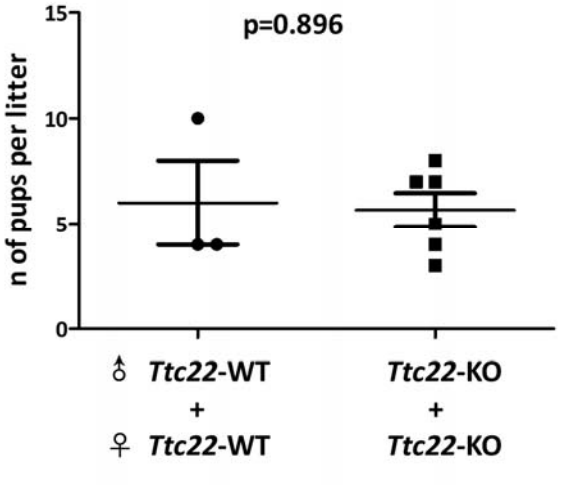

353

354 **Figure 5**. Fertility comparison between *Ttc22*$^{+/+}$ and *Ttc22*$^{-/-}$ mice. Mating pairs were monitored for
355 litter production during the first pregnancy. Three pairs of wild-type (*Ttc22*$^{+/+}$) mice and six pairs of
356 homozygous knockout (*Ttc22*$^{-/-}$) mice were established. Each symbol represents a pair. The data are
357 presented as the mean ± SD.
358

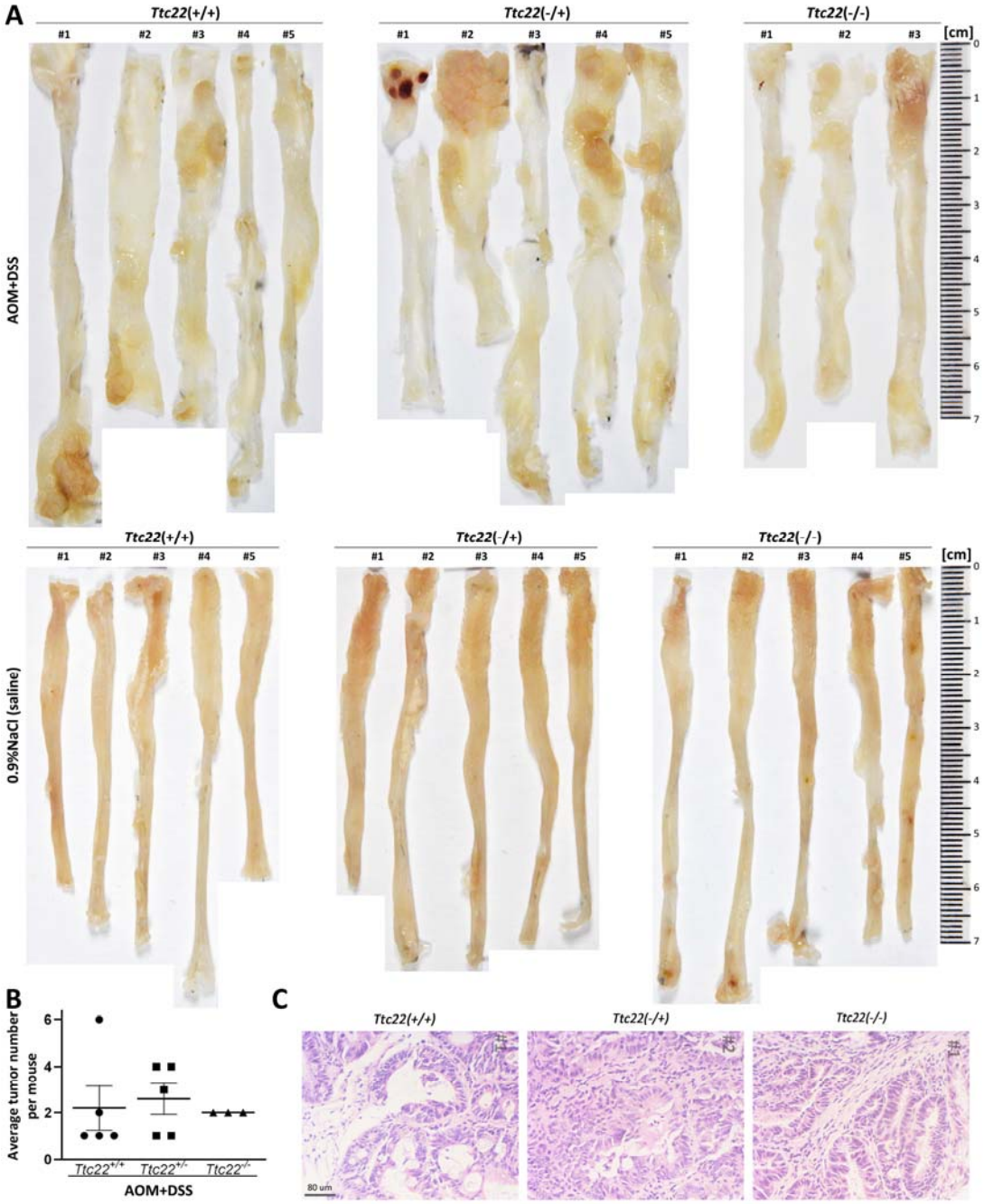

Figure 6. Induction of colon tumors by AOM/DSS in male C57BL mice with different *Ttc22* genotypes. (**A**) Overview of tumors in the prefixed colon; (**B**) Scatter plot showing the average tumor number in the colon per mouse; each dot represents one mouse. The data are presented as the mean ± SD. (**C**) Histological images of representative tumors induced by AOM and DSS.

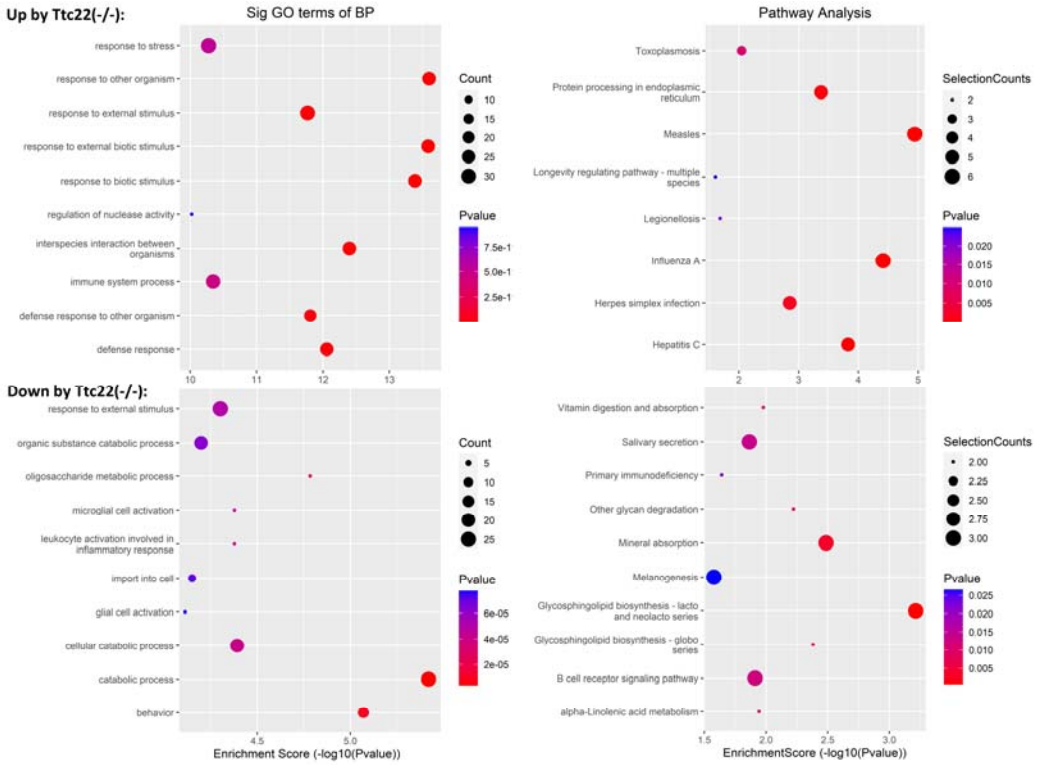

Figure 7. Enrichment scores for genes upregulated and downregulated by homozygous *Ttc22* knockout in the colon of 57-week-old male mice

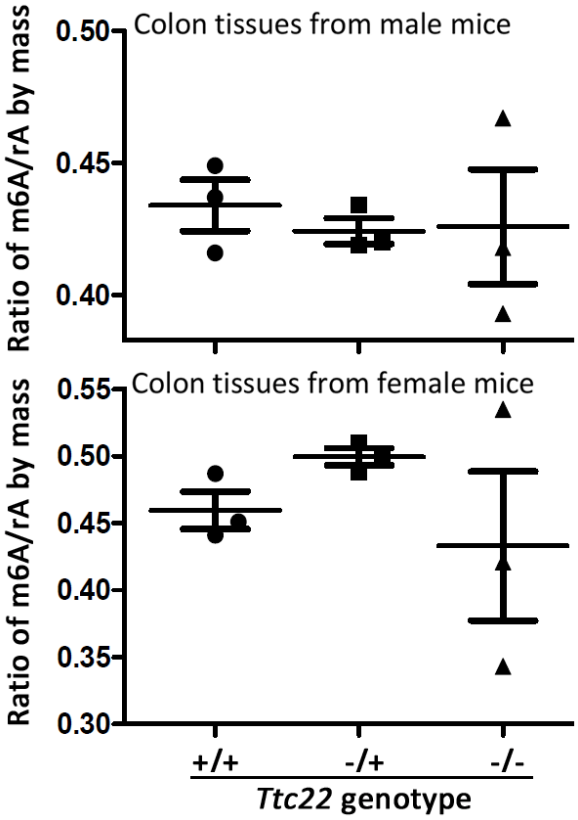

369

370 **Figure 8.** Effect of Ttc22 inactivation on total RNA m6A modification in the colons of mice. The ratio
371 of total m6A to total adenosine in RNA (m6A/rA) in the colon tissues of mice with various *Ttc22*
372 genotypes, as determined by mass.

373

374 ## TABLE LIST

375 **Table 1**. Incidence and latency period of spontaneous tumors* in C57BL/6N mice with different *Ttc22* genotypes

	Male			Female		
Genotype	*n*	Mice with tumor (%)	Range of tumor latent weeks	n	Mice with tumor (%)	Range of tumor latent weeks
Ttc22$^{+/+}$	17	3 (17.6)	45, 55, 77	12	0	-
Ttc22$^{+/-}$	14	2 (14.3)	57, 60	19	4 (21.1)	57, 60, 65, 75
Ttc22$^{-/-}$	27	2 (7.4)	54, 54	39	6 (15.4)	41, 55, 55,55, 59, 60
(sum)	58	7 (12.1)		60	10 (16.7)	

376 * including lymphoma, sebaceous carcinoma, and basal carcinoma